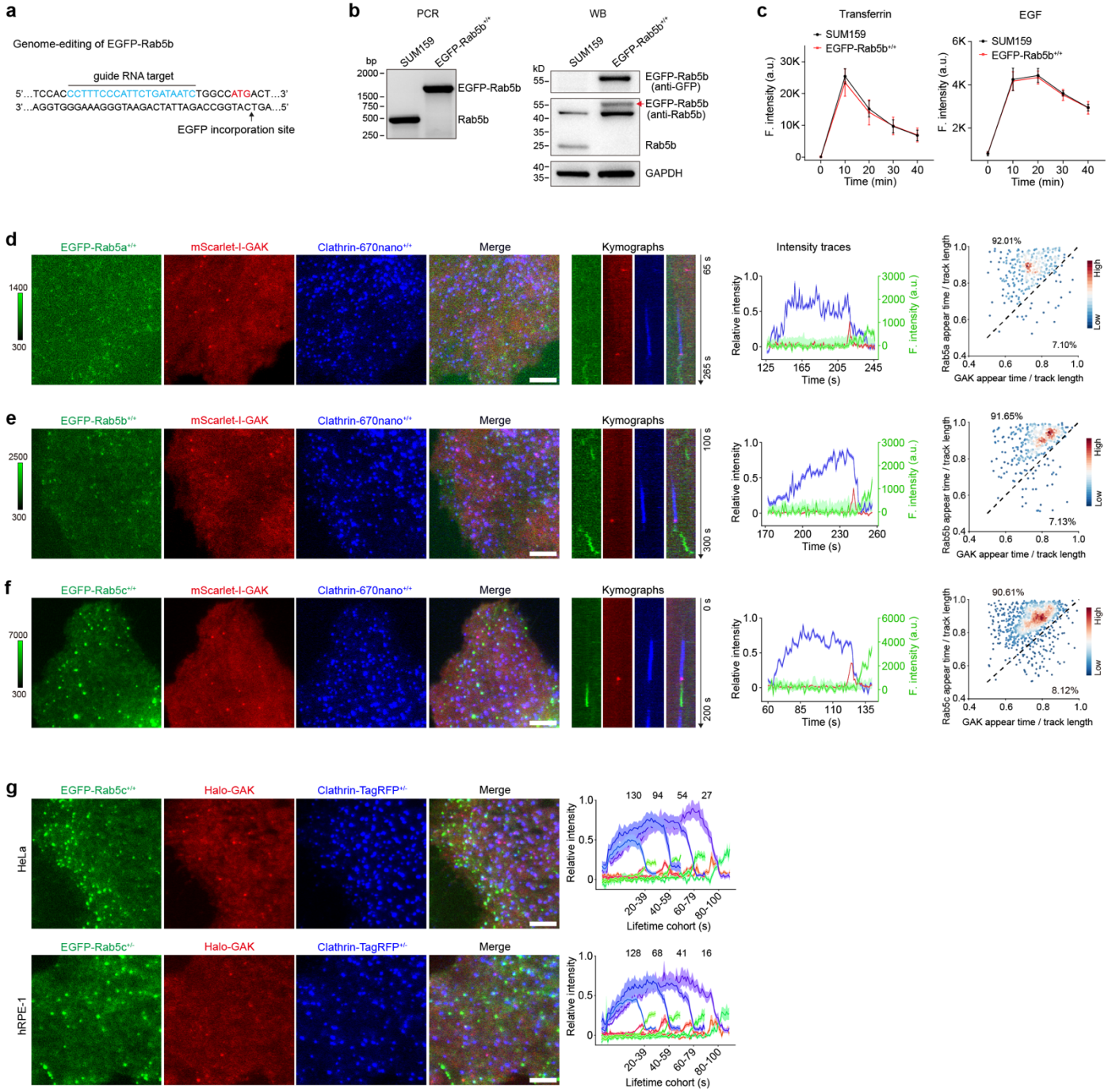


Supplementary Fig. 1. Rab5 is recruited to nascent endocytic vesicles after uncoating in gene-edited cells.

a, The CRISPR/Cas9 genome editing strategy used to incorporate EGFP at the N-terminus of Rab5b. The target sequence at the *RAB5B* genomic locus recognized by the sgRNA and the site of EGFP incorporation upon homologous recombination are highlighted.

b, Left: genomic PCR analysis showing biallelic integration of EGFP into the *RAB5B* genomic locus to generate the clonal gene-edited SUM159 cell line EGFP-Rab5b$^{+/+}$. Right: western blot analysis of cell lysates probed with antibodies against GFP, Rab5b, or GAPDH (loading control).

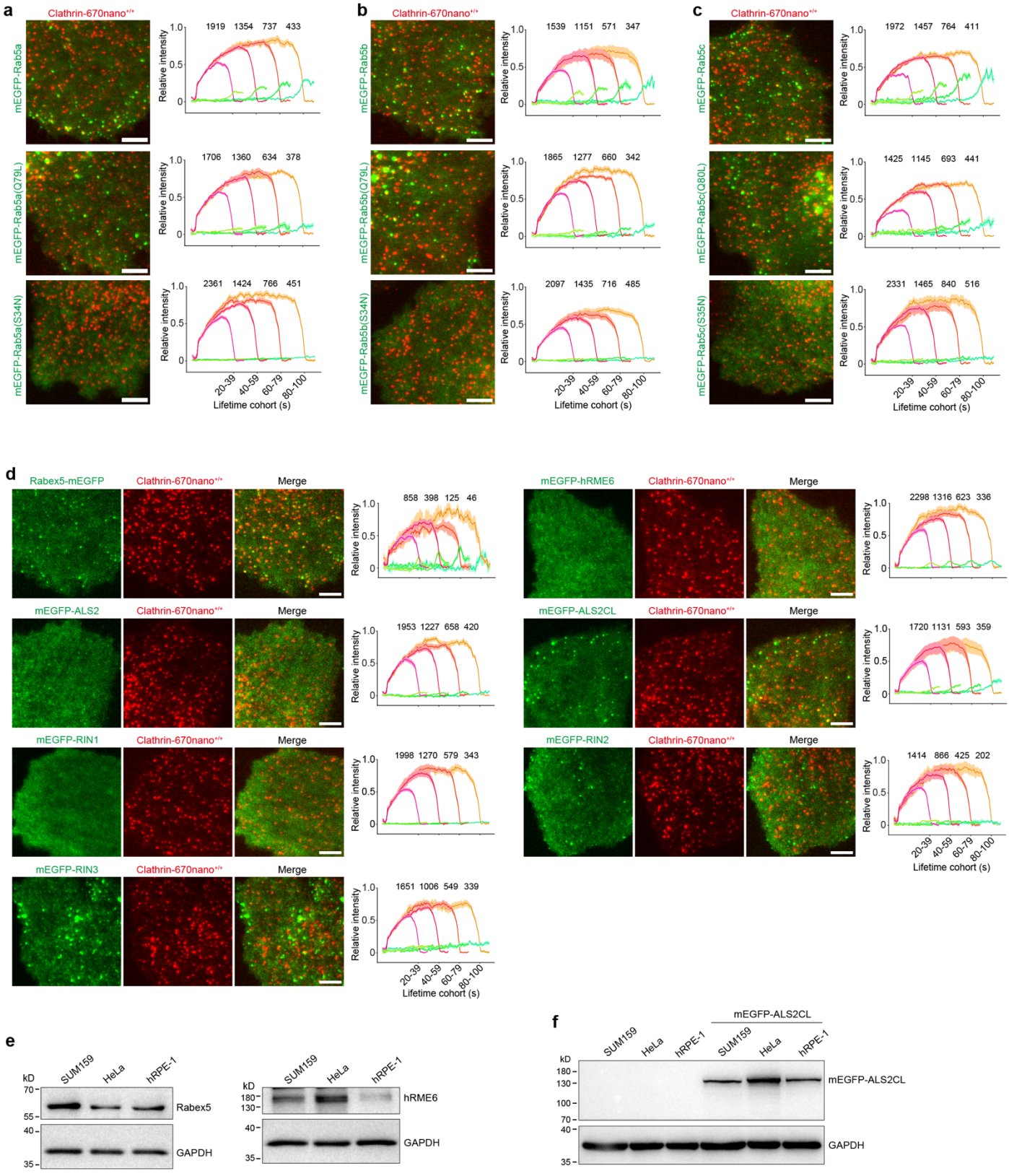
c, Effect of expression of EGFP-Rab5b on receptor-mediated uptake and recycling of transferrin (left) and the uptake and degradation of EGF (right). Flow cytometry was used to probe the amounts of Alexa Fluor 647–conjugated

transferrin and Alexa Fluor 555–conjugated EGF in parental and gene-edited EGFP-Rab5b$^{+/+}$ cells (mean ± SD; n = 3 independent experiments).

d-f, SUM159 cells gene-edited for EGFP-Rab5a$^{+/+}$ and clathrin-670nano$^{+/+}$ (**d**), EGFP-Rab5b$^{+/+}$ and clathrin-670nano$^{+/+}$ (**e**), or EGFP-Rab5c$^{+/+}$ and clathrin-670nano$^{+/+}$ (**f**) were transfected with mScarlet-I-GAK and then imaged at the bottom surface using triple-color TIRF microscopy every 1 s for 300 s. From left to right: a single frame from a representative time series; kymographs and fluorescence (F.) intensity traces of an endocytic event; density scatter plots depicting the normalized appearance times of GAK and Rab5a/b/c (appearance time divided by track length), with the fractions of events above and below the diagonal indicated. The corresponding intensity-lifetime cohorts and the relative timing of GAK and Rab5a/b/c recruitment during clathrin uncoating are presented in **Fig. 1a-c**.

g, Gene-edited HeLa cells expressing EGFP-Rab5c$^{+/+}$ clathrin-TagRFP$^{+/-}$ or hRPE-1 cells expressing EGFP-Rab5c$^{+/-}$ clathrin-TagRFP$^{+/-}$ were transfected with Halo-GAK, stained with the JFX_{650}-HaloTag ligand, and then imaged at the bottom surface by triple-color TIRF microscopy every 1 s for 300 s. From left to right: a single frame from a representative time series; and the intensity-lifetime cohorts (mean ± SEM; 13 HeLa cells and 13 hRPE-1 cells).

Experiments were repeated three times with similar results. Scale bars, 5 μm. Source numerical data are available in source data.



Supplementary Fig. 2. Identification of Rab5-related GEFs recruited to uncoated endocytic carriers.

a-c, Gene-edited clathrin-670nano$^{+/+}$ cells were transfected with mEGFP-tagged wild-type, constitutively GTP-bound, or constitutively GDP-bound forms of Rab5a/b/c, and then imaged by TIRF microscopy every 1 s for 300 s. Snapshots

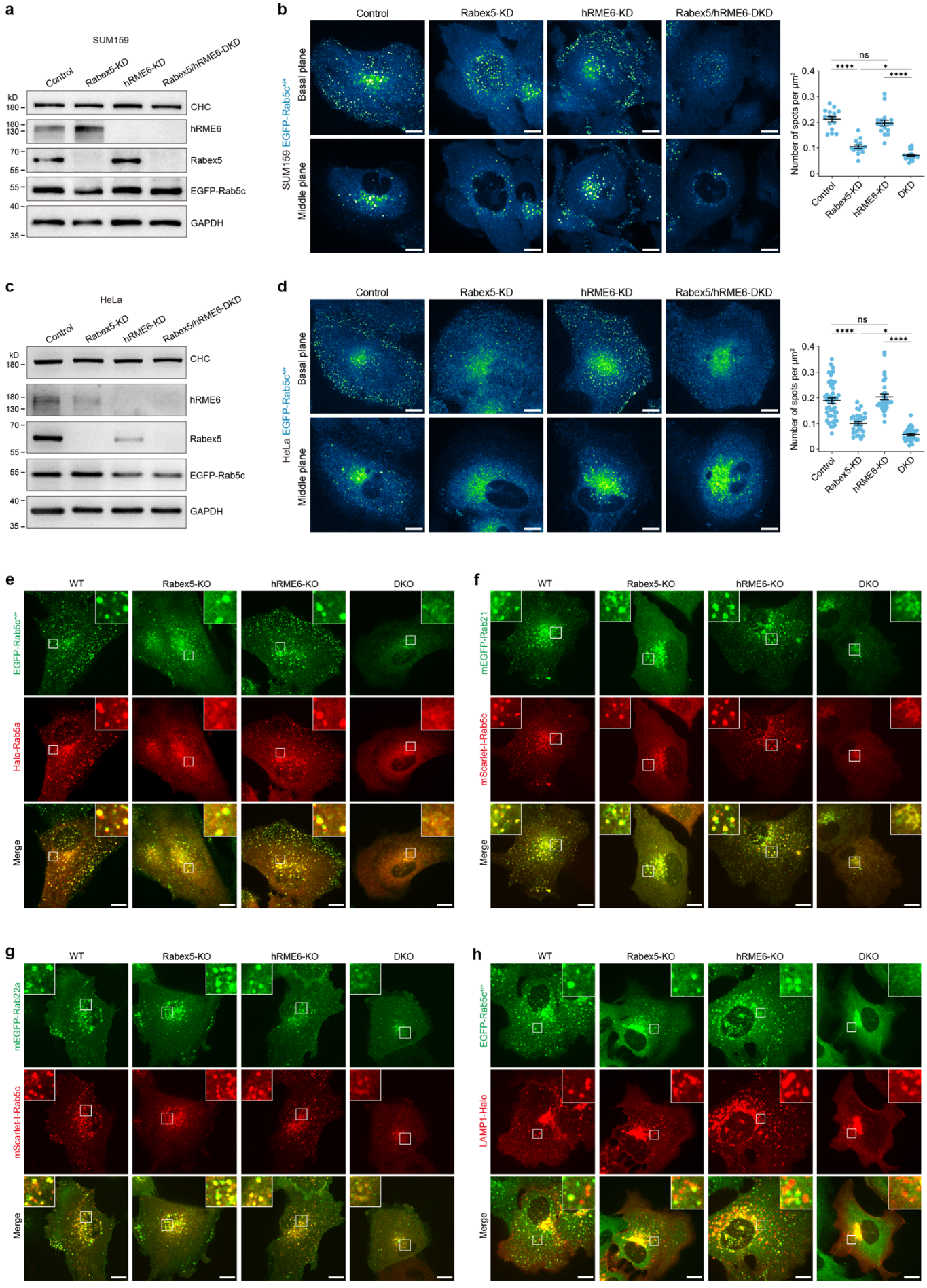
and intensity-lifetime cohorts (mean ± SEM) show recruitment of different forms of Rab5 to nascent endocytic vesicles (10 to 13 cells).

d, Gene-edited SUM159 cells expressing clathrin-670nano$^{+/+}$ were transfected with mEGFP-tagged GEF molecules as indicated and then imaged by TIRF microscopy every 1 s for 300 s. A single frame from a representative time series is presented, together with intensity-lifetime cohorts (mean ± SEM) showing the recruitment of different proteins during endocytic vesicle formation (8 to 10 cells).

e, Expression levels of Rabex5 and hRME6 in SUM159, HeLa, and hRPE-1 cells were examined by western blot analysis using antibodies against GAPDH and Rabex5 or hRME6.

f, Expression of ALS2CL in SUM159, HeLa, and hRPE-1 cells without or with mEGFP-ALS2CL transfection was examined by western blot analysis using antibodies against GAPDH and ALS2CL. The expression of endogenous ALS2CL could not be detected in SUM159, HeLa, and hRPE-1 cells.

Experiments were repeated three times (**a**-**d**, **f**) or twice (**e**) with similar results. Scale bars, 5 μm.


a
SUM159
Control
Rabex5-KD
hRME6-KD
Rabex5/hRME6-DKD
kD
180
CHC
180
130
hRME6
70
55
Rabex5
55
EGFP-Rab5c
40
GAPDH
35
b
Control
Rabex5-KD
hRME6-KD
Rabex5/hRME6-DKD
SUM159 EGFP-Rab5c+/+
Basal plane
Middle plane
ns
****
*
****
Number of spots per µm²
0.4
0.3
0.2
0.1
0
Control
Rabex5-KD
hRME6-KD
DKD
c
HeLa
Control
Rabex5-KD
hRME6-KD
Rabex5/hRME6-DKD
kD
180
CHC
180
130
hRME6
70
55
Rabex5
55
EGFP-Rab5c
40
GAPDH
35
d
Control
Rabex5-KD
hRME6-KD
Rabex5/hRME6-DKD
HeLa EGFP-Rab5c+/+
Basal plane
Middle plane
ns
****
*
****
Number of spots per µm²
0.4
0.3
0.2
0.1
0
Control
Rabex5-KD
hRME6-KD
DKD
e
WT
Rabex5-KO
hRME6-KO
DKO
EGFP-Rab5c+/+
Halo-Rab5a
Merge
f
WT
Rabex5-KO
hRME6-KO
DKO
mEGFP-Rab21
mScarlet-I-Rab5c
Merge
g
WT
Rabex5-KO
hRME6-KO
DKO
mEGFP-Rab22a
mScarlet-I-Rab5c
Merge
h
WT
Rabex5-KO
hRME6-KO
DKO
EGFP-Rab5c+/+
LAMP1-Halo
Merge

Supplementary Fig. 3. Simultaneous elimination of Rabex5 and hRME6 expression impairs Rab5-positive early endosome formation.

a, Gene-edited SUM159 cells expressing EGFP-Rab5c$^{+/+}$ clathrin-TagRFP$^{+/+}$ were treated with control siRNA or with siRNA targeting Rabex5 (Rabex5-KD), hRME6 (hRME6-KD), or both Rabex5 and hRME6 (Rabex5/hRME6-DKD). The expression of the indicated proteins in the siRNA-treated cells was analyzed by western blot. CHC, clathrin heavy chain.

b, The siRNA-treated cells were imaged in 3D using spinning-disk confocal microscopy (imaging planes spaced at 0.35 μm). Left: distribution of EGFP-Rab5c at the bottom surface and the middle plane of the cells. Right: numbers of identified EGFP-Rab5c spots in 15 control, 15 Rabex5-KD, 17 hRME6-KD, and 18 DKD cells (mean ± SEM).

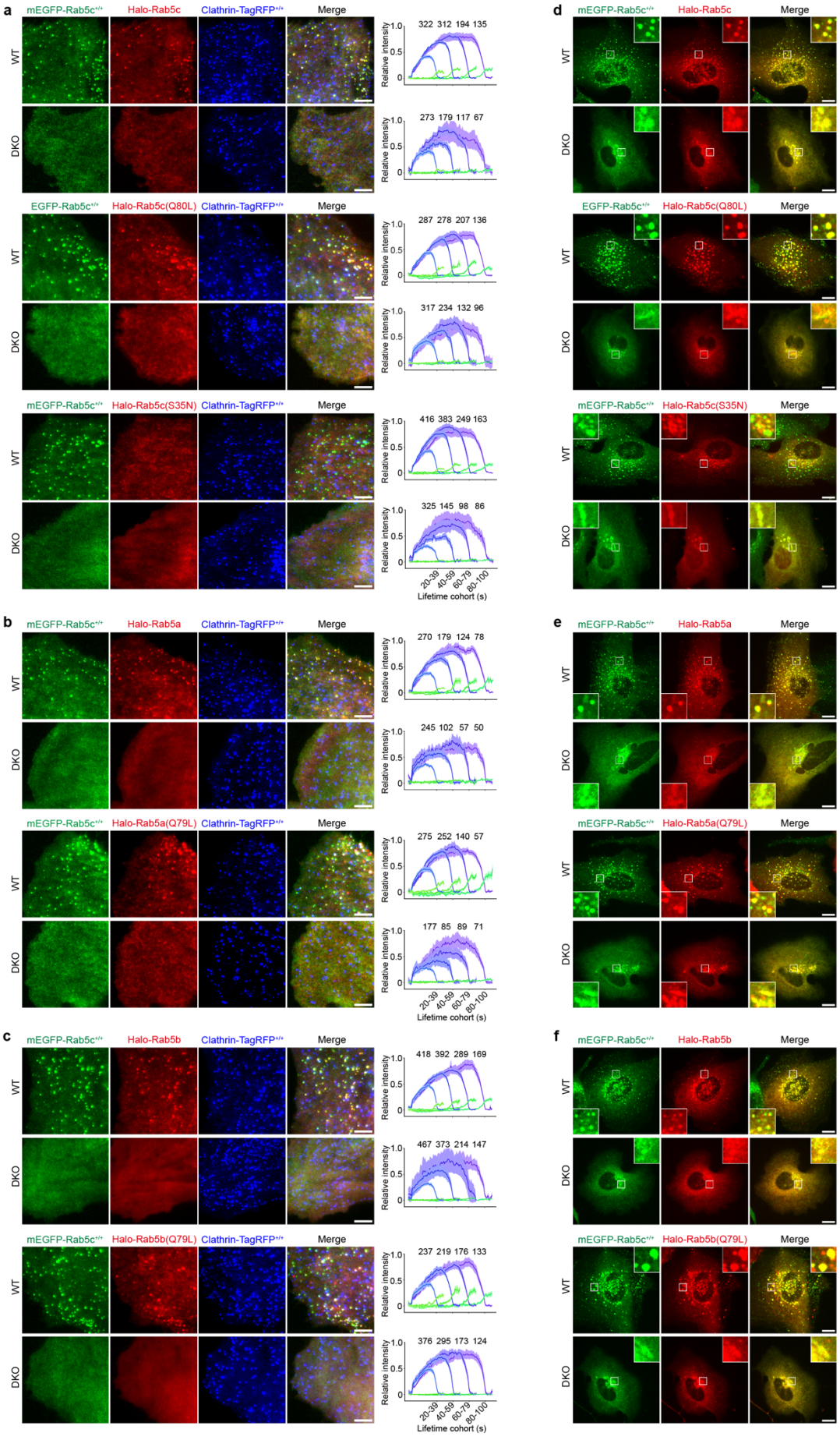
c, **d**, Gene-edited HeLa cells expressing EGFP-Rab5c$^{+/+}$ clathrin-TagRFP$^{+/-}$ were treated with control siRNA or with siRNA targeting Rabex5, hRME6, or both Rabex5 and hRME6. The expression levels of the indicated proteins were assessed by western blot (**c**) and the intracellular distribution of EGFP-Rab5c was imaged and analyzed by spinning-disk confocal microscopy (mean ± SEM; n = 45, 31, 32, and 30 cells) (**d**).

e, Gene-edited EGFP-Rab5c$^{+/+}$ clathrin-TagRFP$^{+/+}$ SUM159 cells lacking Rabex5 and/or hRME6 expression were transiently transfected with Halo-Rab5a, stained with the JFX$_{650}$-HaloTag ligand, and then imaged using spinning-disk confocal microscopy. Representative images show the distribution of EGFP-Rab5c with Halo-Rab5a around the middle plane of the cells.

f, **g**, SUM159 cells lacking Rabex5 and/or hRME6 expression were transiently transfected with mScarlet-I-Rab5c and mEGFP-Rab21 (**f**), or mScarlet-I-Rab5c and mEGFP-Rab22a (**g**), and then imaged using spinning-disk confocal microscopy. Representative images show the distribution of mScarlet-I-Rab5c with mEGFP-Rab21 or mEGFP-Rab22a around the middle plane of the cells.

h, Gene-edited EGFP-Rab5c$^{+/+}$ clathrin-TagRFP$^{+/+}$ SUM159 cells lacking Rabex5 and/or hRME6 expression were transiently transfected with LAMP1-Halo, stained with the JFX$_{650}$-HaloTag ligand, and then imaged using spinning-disk confocal microscopy. Representative images show the distribution of EGFP-Rab5c with LAMP1-Halo around the middle plane of the cells.

Experiments were repeated three times (**a**, **b**, **d**-**h**) or twice (**c**) with similar results. Statistical analysis was performed using the ordinary one-way ANOVA with Tukey's multiple comparisons test; *$P < 0.05$; ****$P < 0.0001$; ns, not significant. Scale bars, 10 μm. Source numerical data are available in source data.

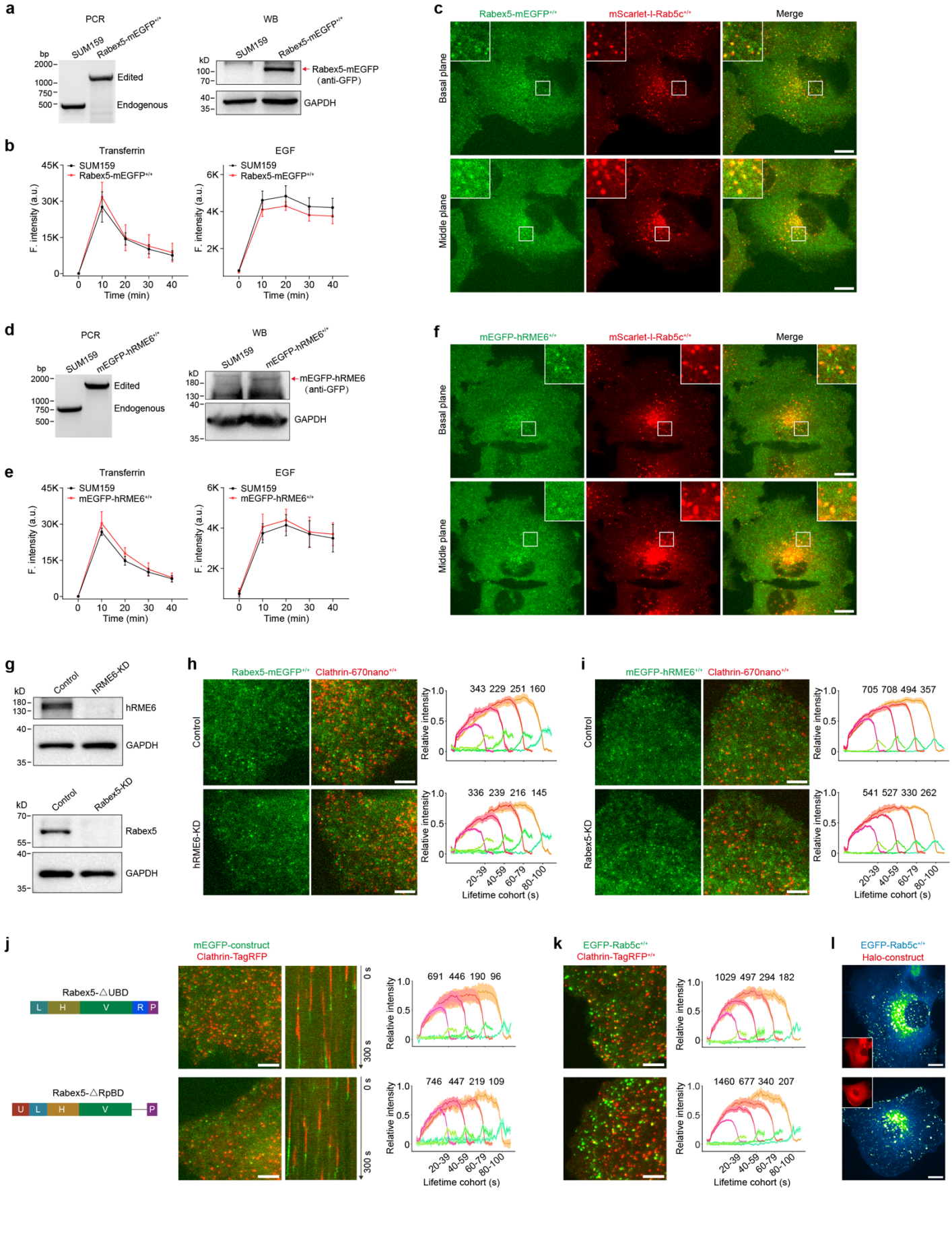

a
mEGFP-Rab5c+/+
Halo-Rab5c
Clathrin-TagRFP+/+
Merge
WT
DKO
322 312 194 135
273 179 117 67
EGFP-Rab5c+/+
Halo-Rab5c(Q80L)
287 278 207 136
317 234 132 96
mEGFP-Rab5c+/+
Halo-Rab5c(S35N)
416 383 249 163
325 145 98 86
Relative intensity
1.0
0.5
0
20-39
40-59
60-79
80-100
Lifetime cohort (s)
b
mEGFP-Rab5c+/+
Halo-Rab5a
Clathrin-TagRFP+/+
Merge
270 179 124 78
245 102 57 50
mEGFP-Rab5c+/+
Halo-Rab5a(Q79L)
275 252 140 57
177 85 89 71
c
mEGFP-Rab5c+/+
Halo-Rab5b
Clathrin-TagRFP+/+
Merge
418 392 289 169
467 373 214 147
mEGFP-Rab5c+/+
Halo-Rab5b(Q79L)
237 219 176 133
376 295 173 124
d
mEGFP-Rab5c+/+
Halo-Rab5c
Merge
EGFP-Rab5c+/+
Halo-Rab5c(Q80L)
mEGFP-Rab5c+/+
Halo-Rab5c(S35N)
e
mEGFP-Rab5c+/+
Halo-Rab5a
Merge
mEGFP-Rab5c+/+
Halo-Rab5a(Q79L)
f
mEGFP-Rab5c+/+
Halo-Rab5b
Merge
mEGFP-Rab5c+/+
Halo-Rab5b(Q79L)

Supplementary Fig. 4. Expression of different forms of Rab5a/b/c fails to restore Rab5 recruitment in the Rabex5/hMRE6-DKO cells.

a-**c**, The WT and Rabex5/hMRE6-DKO EGFP-Rab5c$^{+/+}$ clathrin-TagRFP$^{+/+}$ cells were transfected with the specified Halo-tagged Rab5 mutant, stained with the JFX_{650}-HaloTag ligand, and then imaged by TIRF microscopy every 1 s for 300 s. Shown are a single frame from a representative time series and intensity-lifetime cohorts (mean ± SEM) from 8 to 11 cells.

d-**f**, The WT and Rabex5/hMRE6-DKO EGFP-Rab5c$^{+/+}$ clathrin-TagRFP$^{+/+}$ cells were transfected with the specified Halo-tagged Rab5 mutant, stained with the JFX_{650}-HaloTag ligand, and then imaged in 3D using spinning-disk confocal microscopy (imaging planes spaced at 0.35 μm). The distributions of mEGFP-Rab5c and Halo-tagged Rab5 mutant at the middle plane of the cells are shown.

Experiments were repeated three times (**a**, **c**-**f**) or twice (**b**) with similar results. Scale bars, 5 μm (**a**-**c**) and 10 μm (**d**-**f**).


a
PCR
WB
SUM159
Rabex5-mEGFP+/+
bp
2000
1000
750
500
Edited
Endogenous
kD
100
70
40
35
Rabex5-mEGFP (anti-GFP)
GAPDH
b
Transferrin
EGF
SUM159
Rabex5-mEGFP+/+
F. intensity (a.u.)
45K
30K
15K
0
6K
4K
2K
0 10 20 30 40
Time (min)
c
Rabex5-mEGFP+/+
mScarlet-I-Rab5c+/+
Merge
Basal plane
Middle plane
d
mEGFP-hRME6+/+
180
130
mEGFP-hRME6 (anti-GFP)
e
mEGFP-hRME6+/+
f
mEGFP-hRME6+/+
g
Control
hRME6-KD
hRME6
Rabex5-KD
Rabex5
h
Clathrin-670nano+/+
Relative intensity
1.0
0.5
343 229 251 160
336 239 216 145
20-39
40-59
60-79
80-100
Lifetime cohort (s)
i
705 708 494 357
541 527 330 262
j
mEGFP-construct
Clathrin-TagRFP
Rabex5-△UBD
L H V R P
Rabex5-△RpBD
U L H V P
0 s
300 s
691 446 190 96
746 447 219 109
k
EGFP-Rab5c+/+
Clathrin-TagRFP+/+
1029 497 294 182
1460 677 340 207
l
EGFP-Rab5c+/+
Halo-construct

Supplementary Fig. 5. Distribution and dynamics of Rabex5 and hRME6 in gene-edited cells.

a, Left: genomic PCR analysis showing biallelic integration of mEGFP into the *RABGEF1* genomic locus to generate the clonal gene-edited SUM159 cell line Rabex5-mEGFP$^{+/+}$. Right: western blot analysis of cell lysates probed with antibodies against GFP and GAPDH (loading control).

b, Effect of expression of Rabex5-mEGFP on receptor-mediated uptake and recycling of transferrin (left) and the uptake and degradation of EGF (right). Flow cytometry was used to probe the amounts of Alexa Fluor 647–conjugated transferrin and Alexa Fluor 555–conjugated EGF in parental and gene-edited Rabex5-mEGFP$^{+/+}$ cells (mean ± SD; n = 4 independent experiments).

c, Gene-edited cells expressing Rabex5-mEGFP$^{+/+}$ mScarlet-I-Rab5c$^{+/+}$ were imaged in 3D by spinning-disk confocal microscopy (imaging planes spaced at 0.35 μm). The distributions of Rabex5-mEGFP and mScarlet-I-Rab5c at the bottom surface and the middle plane of the cells are shown.

d, Left: genomic PCR analysis showing biallelic integration of mEGFP into the *GAPVD1* genomic locus to generate the clonal gene-edited SUM159 cell line mEGFP-hRME6$^{+/+}$. Right: western blot analysis of cell lysates probed with antibodies against GFP and GAPDH (loading control).

e, Effect of expression of mEGFP-hRME6 on receptor-mediated uptake and recycling of transferrin (left) and the uptake and degradation of EGF (right). Flow cytometry was used to probe the amounts of Alexa Fluor 647–conjugated transferrin and Alexa Fluor 555–conjugated EGF in parental and gene-edited mEGFP-hRME6$^{+/+}$ cells (mean ± SD; n = 3 independent experiments).

f, Gene-edited cells expressing mEGFP-hRME6$^{+/+}$ mScarlet-I-Rab5c$^{+/+}$ were imaged in 3D by spinning-disk confocal microscopy (imaging planes spaced at 0.35 μm). The distributions of mEGFP-hRME6 and mScarlet-I-Rab5c at the bottom surface and the middle plane of the cells are shown.

g, Top: gene-edited cells expressing Rabex5-mEGFP$^{+/+}$ clathrin-670nano$^{+/+}$ were treated with either control siRNA or siRNA targeting hRME6 (hRME6-KD). Reduction in the expression of hRME6 in the hRME6-KD cells was confirmed by western blot analysis. Bottom: gene-edited cells expressing mEGFP-hRME6$^{+/+}$ clathrin-670nano$^{+/+}$ were treated with either control siRNA or siRNA targeting Rabex5 (Rabex5-KD). The reduction in Rabex5 expression in the Rabex5-KD cells was confirmed by western blot analysis.

h, The siRNA-treated cells were imaged at the bottom surfaces by TIRF microscopy every 1 s for 300 s. A single frame from a representative time series and intensity-lifetime cohorts from 12 control and 12 hRME6-KD cells.

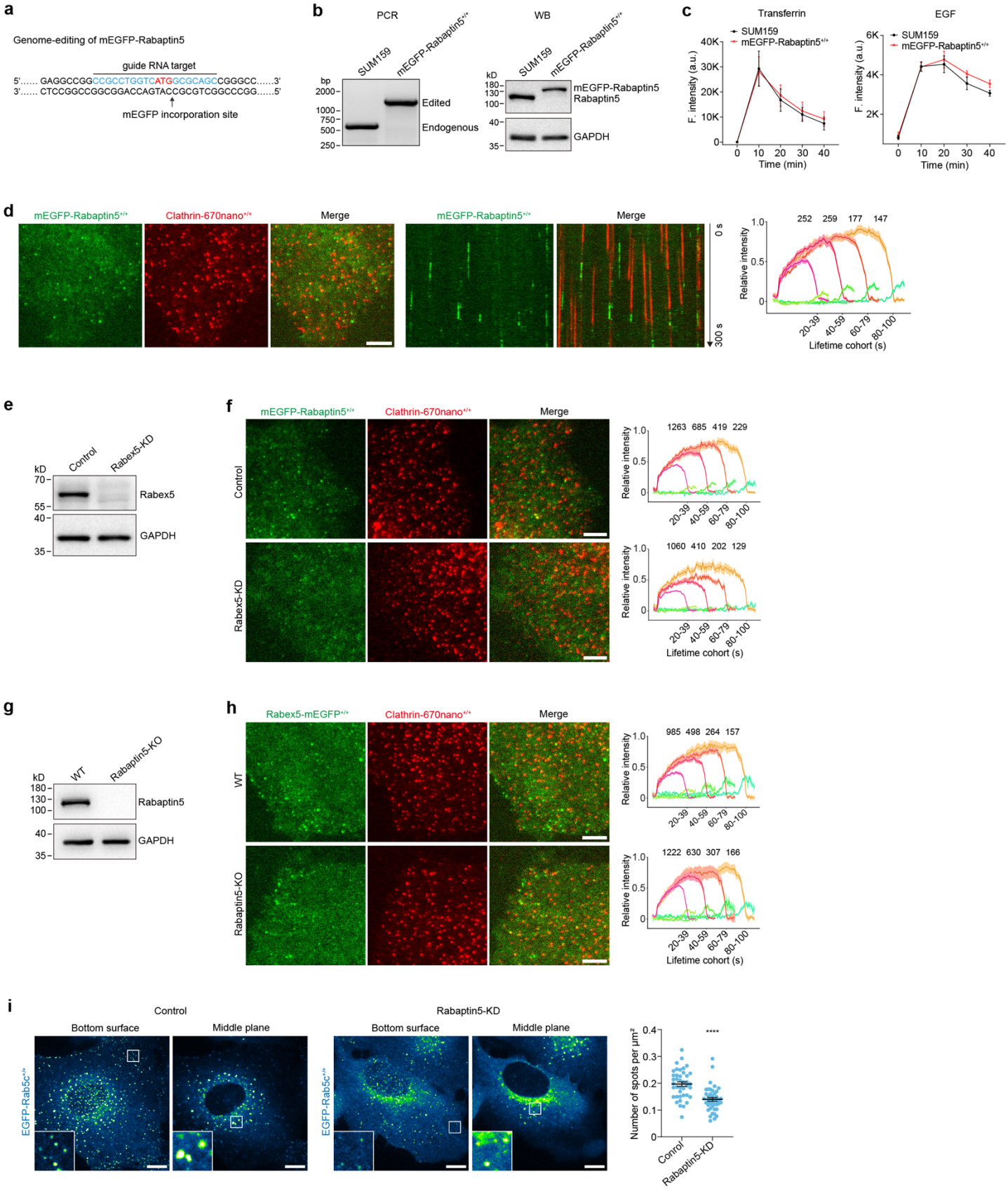
i, The siRNA-treated cells were imaged at the bottom surfaces by TIRF microscopy every 1 s for 300 s. A single frame from a representative time series and intensity-lifetime cohorts from 12 control and 12 Rabex5-KD cells.

j, SUM159 cells with Rabex5-KO were transiently transfected with clathrin-TagRFP and the specified mEGFP-tagged constructs and then imaged by TIRF microscopy every 1 s for 300 s. Left to right: schematic representation of the domain organization of the two constructs; a single frame from a representative time series; kymographs from a representative time series; and intensity-lifetime cohorts from 8 and 9 cells.

k, EGFP-Rab5c$^{+/+}$ clathrin-TagRFP$^{+/+}$ cells with Rabex5/hMRE6-DKO were transiently transfected with the Halo-tagged constructs in (**j**) and then imaged by TIRF microscopy every 1 s for 300 s. Shown are a single frame from a representative time series and the intensity-lifetime cohorts from 10 and 10 cells.

l, EGFP-Rab5c$^{+/+}$ clathrin-TagRFP$^{+/+}$ cells with Rabex5/hMRE6-DKO were transiently transfected with the Halo-tagged constructs in (**j**), stained with the JFX_{650}-HaloTag ligand, and then imaged in 3D by spinning-disk confocal microscopy (imaging planes spaced at 0.35 μm). Shown are maximum-intensity Z projections compiled from four sequential optical sections (starting from the bottom surface) of EGFP-Rab5c and Halo-tagged construct (corner).

Experiments were repeated three (**a**, **c**-**g**, **k**) or four times (**b**, **j**), or twice (**h**, **i**, **l**) with similar results. Data are shown as mean ± SEM in (**h**-**k**). Scale bars, 10 μm in (**c**), (**f**), and (**l**), and 5 μm in (**h**-**k**). Source numerical data are available in source data.


a
Genome-editing of mEGFP-Rabaptin5
guide RNA target
5'..... GAGGCCGGCCGCCTGGTCATGGCGCAGCCGGGCC.....3'
3'..... CTCCGGCCGGCGGACCAGTACCGCGTCGGCCCGG.....5'
mEGFP incorporation site
b
PCR
SUM159
mEGFP-Rabaptin5+/+
bp
2000
1000
750
500
250
Edited
Endogenous
WB
kD
180
130
100
40
35
mEGFP-Rabaptin5
Rabaptin5
GAPDH
c
Transferrin
EGF
SUM159
mEGFP-Rabaptin5+/+
F. intensity (a.u.)
Time (min)
d
mEGFP-Rabaptin5+/+
Clathrin-670nano+/+
Merge
0 s
300 s
Relative intensity
252 259 177 147
20-39 40-59 60-79 80-100
Lifetime cohort (s)
e
Control
Rabex5-KD
Rabex5
GAPDH
f
Control
Rabex5-KD
1263 685 419 229
1060 410 202 129
g
WT
Rabaptin5-KO
h
Rabex5-mEGFP+/+
985 498 264 157
1222 630 307 166
i
Control
Rabaptin5-KD
Bottom surface
Middle plane
EGFP-Rab5c+/+
Number of spots per µm²
****
Conrol
Rabaptin5-KD

Supplementary Fig. 6. Rabaptin5 is not required for Rabex5 recruitment to uncoated endocytic carriers.

a, The CRISPR/Cas9 gene editing strategy used to incorporate mEGFP at the N-terminus of Rabaptin5.

b, Left: genomic PCR analysis showing biallelic integration of mEGFP into the *RABEP1* genomic locus to generate the clonal gene-edited SUM159 cell line mEGFP-Rabaptin5$^{+/+}$. Right: western blot analysis of cell lysates probed with antibodies against Rabaptin5 and GAPDH (loading control).

c, Effect of mEGFP-Rabaptin5 expression on receptor-mediated uptake and recycling of transferrin (left) and the uptake and degradation of EGF (right). Flow cytometry was used to probe the amounts of Alexa Fluor 647–conjugated transferrin and Alexa Fluor 555–conjugated EGF in parental and gene-edited mEGFP-Rabaptin5$^{+/+}$ cells (mean ± SD; n = 3 independent experiments).

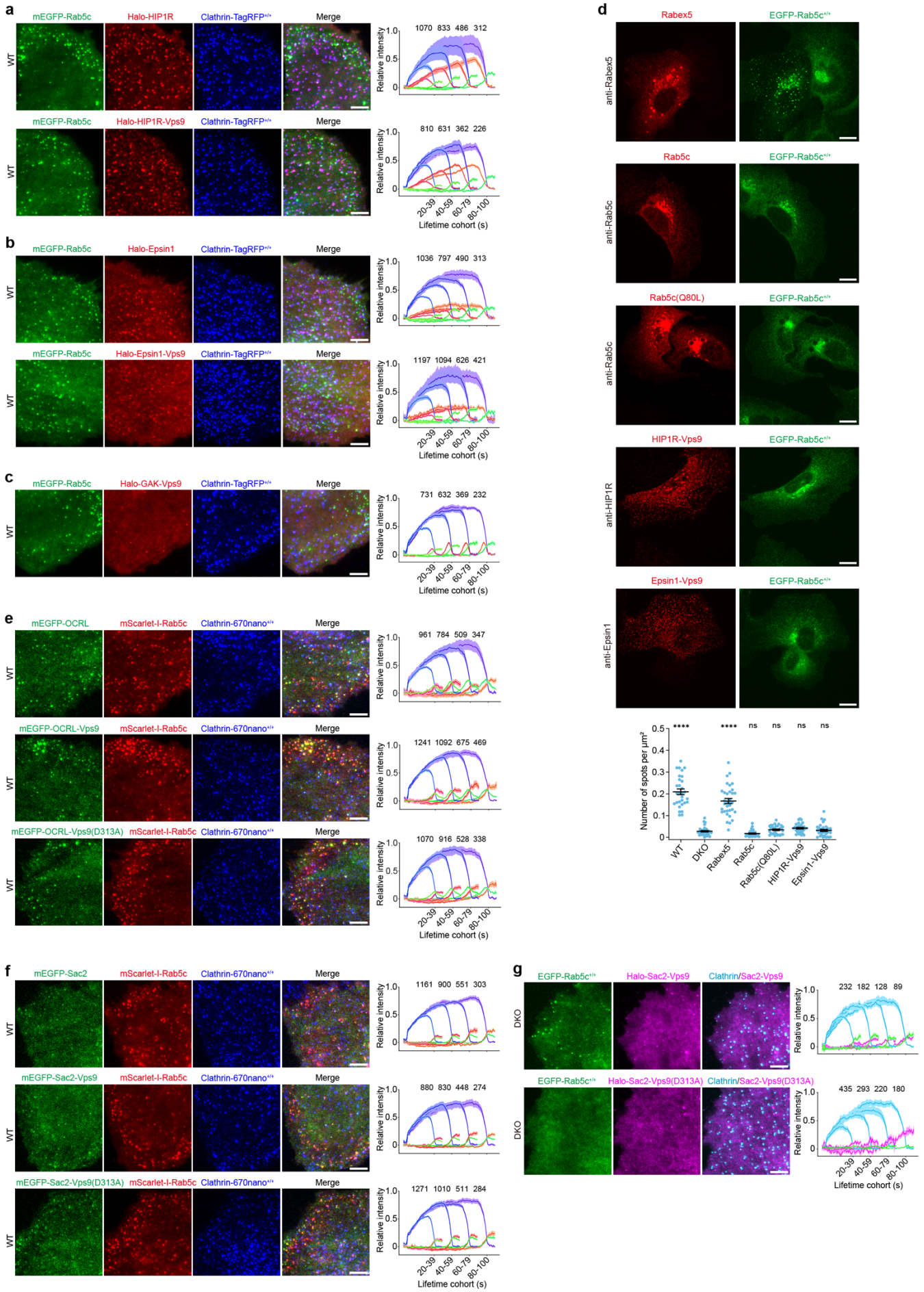
d, mEGFP-Rabaptin5$^{+/+}$ clathrin-670nano$^{+/+}$ cells were imaged at the bottom surface by TIRF microscopy every 1 s for 300 s. From left to right: a single frame from a representative time series; kymographs from a representative time series; and intensity-lifetime cohorts from 12 cells.

e, **f**, mEGFP-Rabaptin5$^{+/+}$ clathrin-670nano$^{+/+}$ cells were treated with either control siRNA or siRNA targeting Rabex5 (Rabex5-KD). The reduction in Rabex5 expression in the Rabex5-KD cells was confirmed by western blot analysis (**e**). The siRNA-treated cells were imaged at the bottom surfaces by TIRF microscopy every 1 s for 300 s. Show is a single frame from a representative time series and intensity-lifetime cohorts from 11 control and 10 Rabex5-KD cells (**f**).

g, **h**, Rabex5-mEGFP$^{+/+}$ clathrin-670nano$^{+/+}$ cells were knocked out for the expression of Rabaptin5 (Rabaptin5-KO), as confirmed by western blot analysis (**g**). WT and Rabaptin5-KO cells were imaged at the bottom surfaces by TIRF microscopy every 1 s for 300 s. Show is a single frame from a representative time series and intensity-lifetime cohorts from 10 WT and 10 Rabaptin5-KO cells (**h**).

i, EGFP-Rab5c$^{+/+}$ clathrin-TagRFP$^{+/+}$ cells were treated with either control siRNA or siRNA targeting Rabaptin5 (Rabaptin5-KD), and then imaged in 3D by spinning-disk confocal microscopy (imaging planes spaced at 0.35 μm). Left: distribution of EGFP-Rab5c at the bottom and middle planes of the cells. Right: number of identified EGFP-Rab5c spots in 40 control cells and 42 Rabaptin5-KD cells. Statistical analysis was performed using the two-tailed unpaired Student's *t*-test; ****$P < 0.0001$.

Experiments were repeated three times with similar results. Data are shown as mean ± SEM in (**d**), (**f**), (**h**), and (**i**). Scale bars, 5 μm in (**d**), (**f**), and (**h**), and 10 μm in (**i**). Source numerical data are available in source data.


a
mEGFP-Rab5c
Halo-HIP1R
Clathrin-TagRFP+/+
Merge
WT
1070 833 486 312
Halo-HIP1R-Vps9
810 631 362 226
b
Halo-Epsin1
1036 797 490 313
Halo-Epsin1-Vps9
1197 1094 626 421
c
Halo-GAK-Vps9
731 632 369 232
e
mEGFP-OCRL
mScarlet-I-Rab5c
Clathrin-670nano+/+
961 784 509 347
mEGFP-OCRL-Vps9
1241 1092 675 469
mEGFP-OCRL-Vps9(D313A)
1070 916 528 338
f
mEGFP-Sac2
1161 900 551 303
mEGFP-Sac2-Vps9
880 830 448 274
mEGFP-Sac2-Vps9(D313A)
1271 1010 511 284
Relative intensity
1.0
0.5
0
20-39
40-59
60-79
80-100
Lifetime cohort (s)
d
Rabex5
EGFP-Rab5c+/+
anti-Rabex5
Rab5c
anti-Rab5c
Rab5c(Q80L)
HIP1R-Vps9
anti-HIP1R
Epsin1-Vps9
anti-Epsin1
Number of spots per μm²
0.5
0.4
0.3
0.2
0.1
0
****
****
ns
ns
ns
ns
WT
DKO
Rabex5
Rab5c
Rab5c(Q80L)
HIP1R-Vps9
Epsin1-Vps9
g
EGFP-Rab5c+/+
Halo-Sac2-Vps9
Clathrin/Sac2-Vps9
DKO
232 182 128 89
Halo-Sac2-Vps9(D313A)
Clathrin/Sac2-Vps9(D313A)
435 293 220 180

Supplementary Fig. 7. Distribution of Rab5 in cells with mistargeted Vps9 or Vps9(D313A).

a-**c**, Gene-edited clathrin-TagRFP$^{+/+}$ cells were transfected with mEGFP-Rab5c and the indicated Halo-tagged constructs, stained with the JFX$_{650}$-HaloTag ligand, and then imaged by TIRF microscopy every 1 s for 300 s. Shown are a single frame from a representative time series and the intensity-lifetime cohorts from 10 to 12 cells.

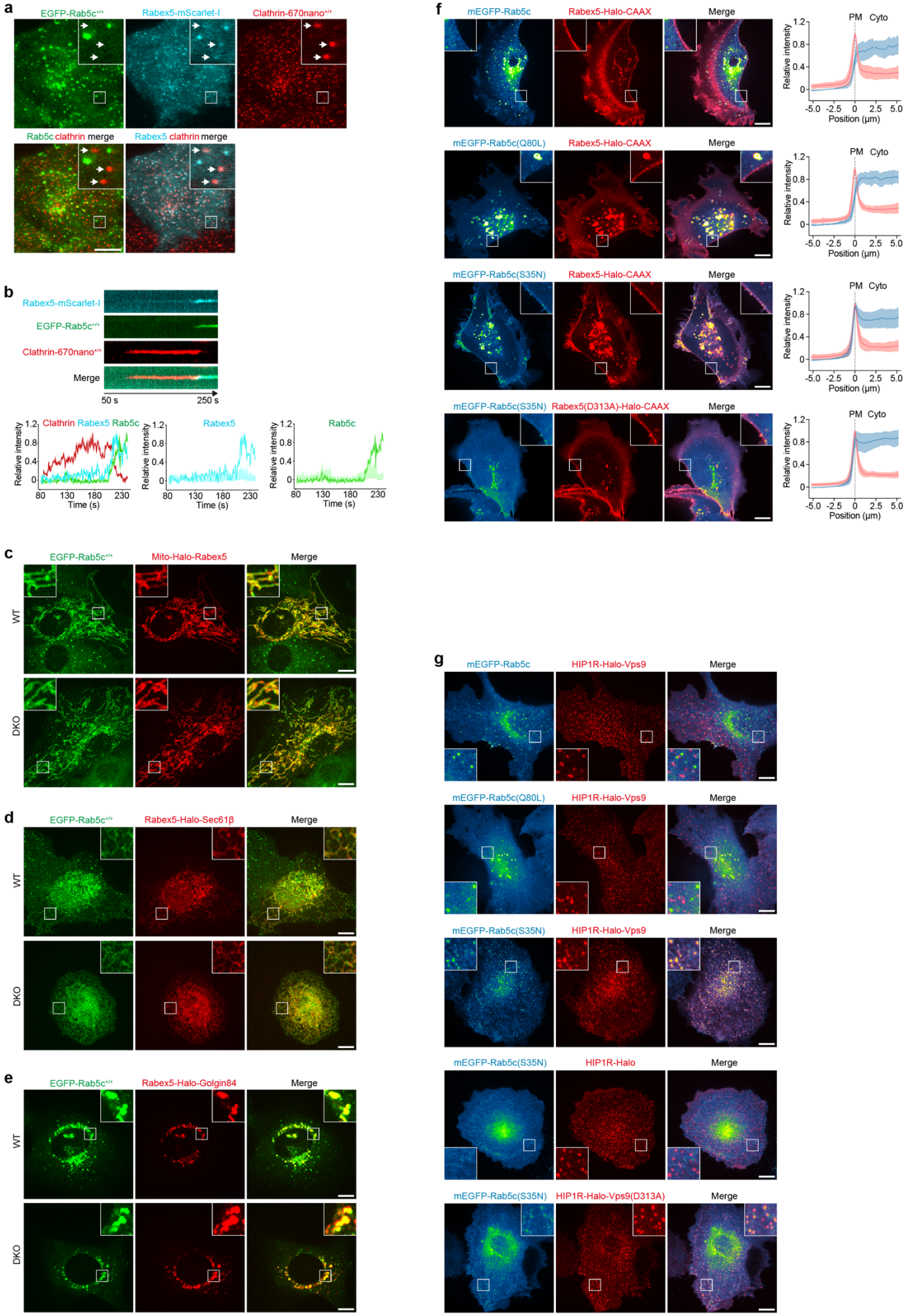
d, Gene-edited EGFP-Rab5c$^{+/+}$ clathrin-TagRFP$^{+/+}$ cells with Rabex5/hMRE6-DKO were transfected with plasmids expressing tag-free Rabex5, Rab5c, Rab5c(Q80L), HIP1R-Vps9, or Epsin1-Vps9. The cells were then stained with the indicated antibodies and imaged by spinning-disk confocal microscopy. The images show the intracellular distribution of EGFP-Rab5c and the over-expressed proteins. The number of EGFP-Rab5c spots identified in WT cells, DKO cells, and DKO cells overexpressing the indicated proteins is quantified below (n = 30, 33, 34, 30, 32, 31, and 33 cells).

e, Gene-edited clathrin-670nano$^{+/+}$ cells were transfected with mScarlet-I-Rab5c and mEGFP-OCRL, mEGFP-OCRL-Vps9, or mEGFP-OCRL-Vps9(D313A), and then imaged by TIRF microscopy every 1 s for 300 s. Shown are a single frame from a representative time series and the intensity-lifetime cohorts from 11, 11 and 10 cells.

f, Clathrin-670nano$^{+/+}$ cells were transfected with mScarlet-I-Rab5c and mEGFP-Sac2, mEGFP-Sac2-Vps9, or mEGFP-Sac2-Vps9(D313A), and then imaged by TIRF microscopy every 1 s for 300 s. Shown are a single frame from a representative time series and the intensity-lifetime cohorts from 12, 11 and 12 cells.

g, EGFP-Rab5c$^{+/+}$ clathrin-TagRFP$^{+/+}$ cells with Rabex5/hMRE6-DKO were transfected with Halo-Sac2-Vps9 or Halo-Sac2-Vps9(D313A), stained with the JFX$_{650}$-HaloTag ligand, and then imaged by TIRF microscopy every 1 s for 300 s. Shown are a single frame from a representative time series and the intensity-lifetime cohorts from 10 and 11 cells.

Experiments were repeated twice (**a**-**c**, **e**, **f**) or three times (**d**, **g**) with similar results. Data are shown as mean ± SEM in (**a**-**g**). Statistical analysis was performed using the ordinary one-way ANOVA, followed by Dunnett's multiple comparisons test with the DKO group in (**d**); ****$P < 0.0001$; ns, not significant. Scale bars, 5 μm in (**a**-**c**) and (**e**-**g**), and 10 μm in (**d**). Source numerical data are available in source data.


a
EGFP-Rab5c+/+
Rabex5-mScarlet-I
Clathrin-670nano+/+
Rab5c clathrin merge
Rabex5 clathrin merge
b
Rabex5-mScarlet-I
EGFP-Rab5c+/+
Clathrin-670nano+/+
Merge
50 s
250 s
Clathrin Rabex5 Rab5c
Rabex5
Rab5c
Relative intensity
Time (s)
c
EGFP-Rab5c+/+
Mito-Halo-Rabex5
Merge
WT
DKO
d
EGFP-Rab5c+/+
Rabex5-Halo-Sec61β
Merge
WT
DKO
e
EGFP-Rab5c+/+
Rabex5-Halo-Golgin84
Merge
WT
DKO
f
mEGFP-Rab5c
Rabex5-Halo-CAAX
Merge
mEGFP-Rab5c(Q80L)
Rabex5-Halo-CAAX
Merge
mEGFP-Rab5c(S35N)
Rabex5-Halo-CAAX
Merge
mEGFP-Rab5c(S35N)
Rabex5(D313A)-Halo-CAAX
Merge
PM Cyto
Relative intensity
Position (μm)
g
mEGFP-Rab5c
HIP1R-Halo-Vps9
Merge
mEGFP-Rab5c(Q80L)
HIP1R-Halo-Vps9
Merge
mEGFP-Rab5c(S35N)
HIP1R-Halo-Vps9
Merge
mEGFP-Rab5c(S35N)
HIP1R-Halo
Merge
mEGFP-Rab5c(S35N)
HIP1R-Halo-Vps9(D313A)
Merge

Supplementary Fig. 8. Mistargeted Rabex5 recruited Rab5 to mitochondria, ER, and Golgi, but not to clathrin-coated pits.

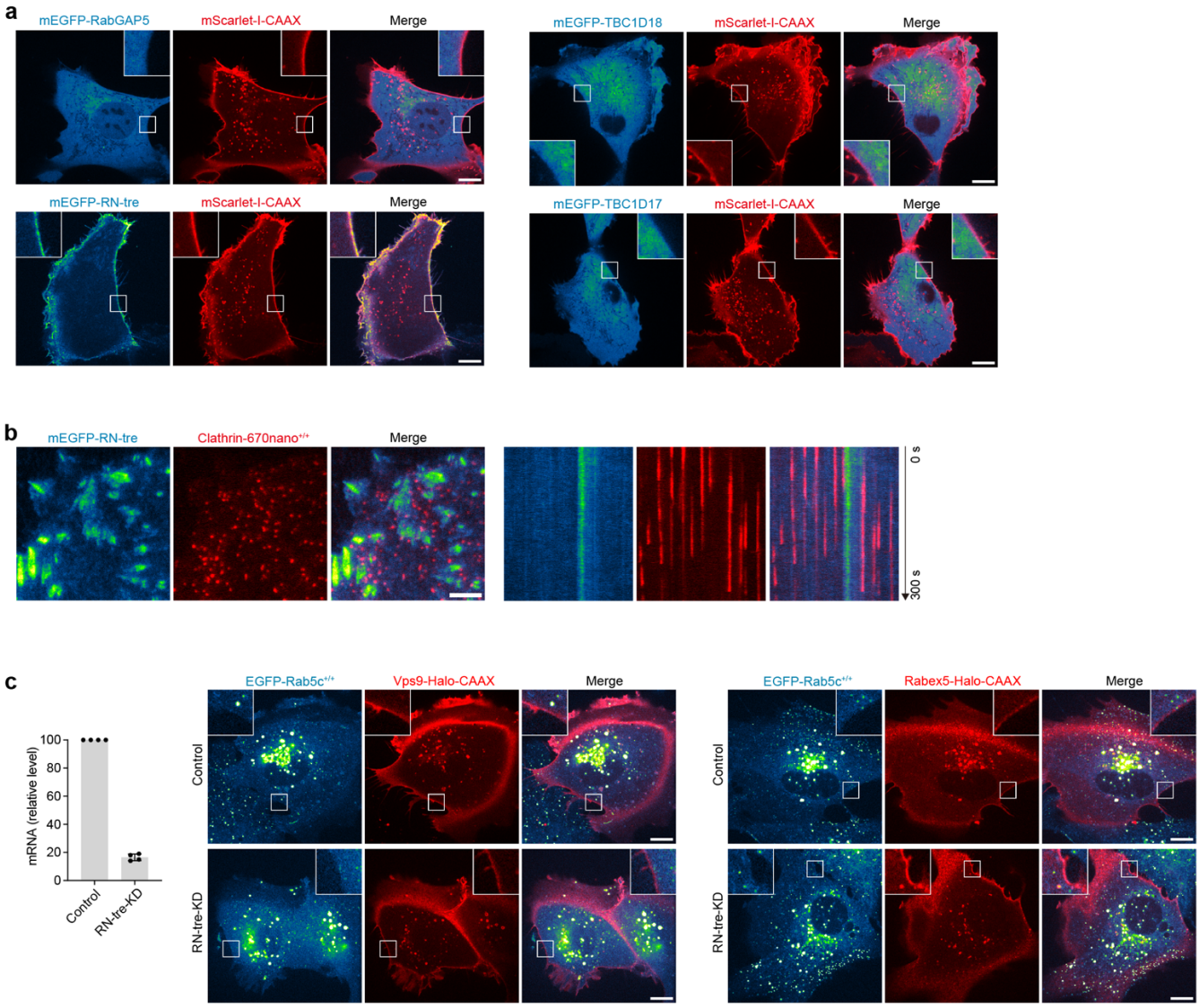
a, **b**, Gene-edited EGFP-Rab5c$^{+/+}$ clathrin-670nano$^{+/+}$ cells were transiently expressed with Rabex5-mScarlet-I, and then imaged by TIRF microscopy. A single frame from a representative time series (**a**). Kymographs and fluorescence intensity traces of one endocytic event (**b**). Local background (thin lines) and significance threshold above background (~2 SD, light shade) are shown in the intensity traces of Rabex5-mScarlet-I (middle) and EGFP-Rab5c (right) (**b**).

c-e, WT and Rabex5/hMRE6-DKO EGFP-Rab5c$^{+/+}$ clathrin-TagRFP$^{+/+}$ cells were transfected with the indicated Halo-tagged constructs, stained with the JFX$_{650}$-HaloTag ligand, and then imaged using spinning-disk confocal microscopy.

f, SUM159 cells were transfected with the indicated mEGFP-tagged Rab5c variants and Rabex5-Halo-CAAX or Rabex5(D313A)-Halo-CAAX, stained with the JFX$_{650}$-HaloTag ligand, and then imaged by spinning-disk confocal microscopy. Images show the distribution of mEGFP-tagged Rab5c variants and Halo-tagged constructs at the middle plane of the cells. Plots show the relative fluorescence intensities of mEGFP-tagged Rab5 variants and Halo-tagged constructs around the plasma membrane of the cells (n = 23, 21, 28, and 29 cells; mean ± SD).

g, SUM159 cells were transiently transfected with the indicated mEGFP-tagged Rab5c variants and Halo-tagged HIP1R variants, stained with the JFX$_{650}$-HaloTag ligand, and then imaged by spinning-disk confocal microscopy. Images show the distribution of Rab5c and HIP1R variants near the bottom surface of the cells.

Experiments were repeated three (**a**-**f**) or four times (**g**) with similar results. Scale bars, 10 μm.



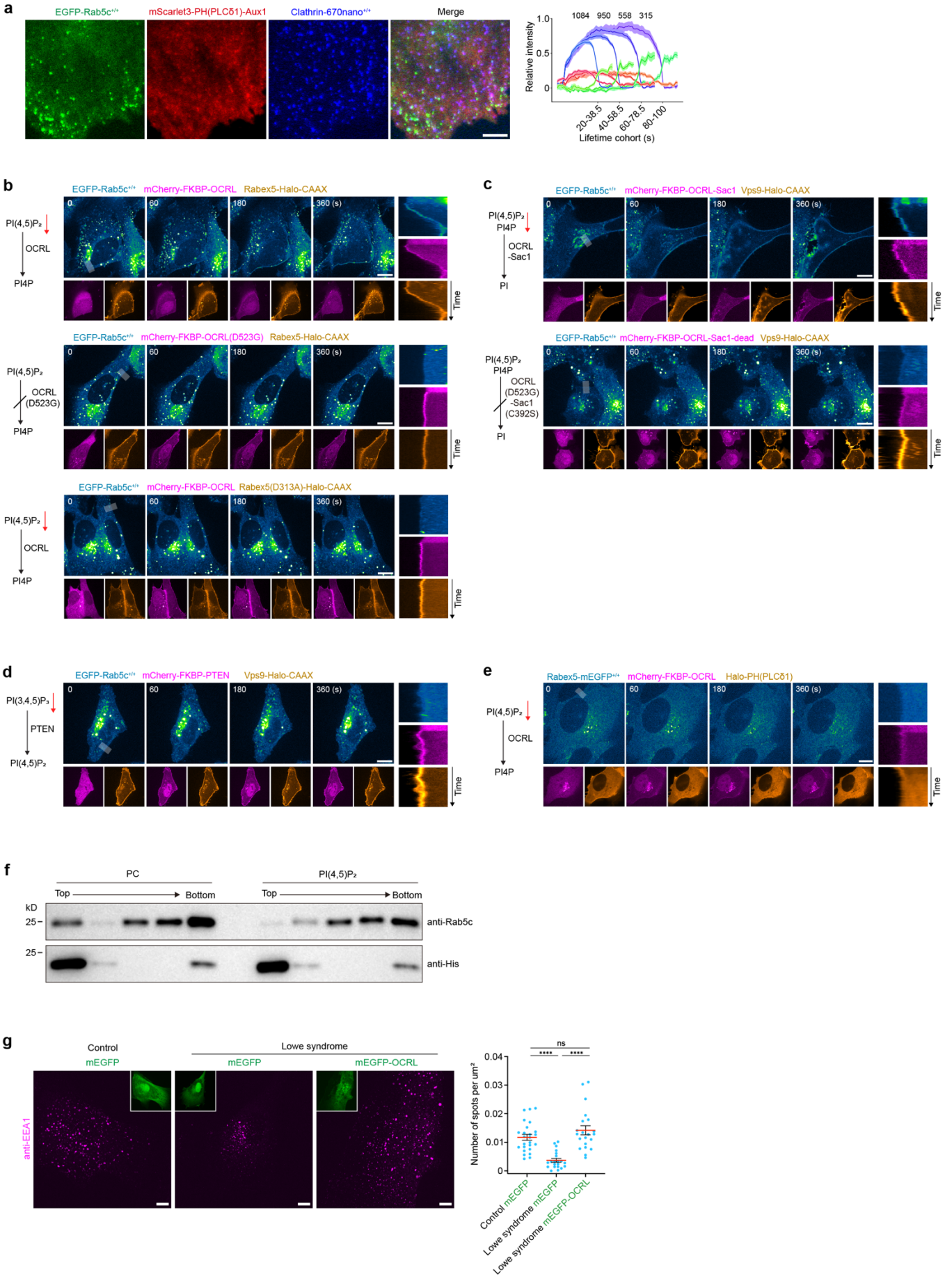
Supplementary Fig. 9. Failure of Rab5 recruitment to plasma membrane-targeted Rabex5 or its Vps9 domain is not related to GAP proteins.

a, SUM159 cells were transfected with mScarlet-I-CAAX and mEGFP-tagged GAPs, and then imaged by spinning-disk confocal microscopy. Images show the distribution of mEGFP-tagged GAPs at the middle plane of the cells.

b, Gene-edited clathrin-670nano$^{+/+}$ cells were transfected with mEGFP-RN-tre and then imaged at the bottom surface using TIRF microscopy every 1 s for 300 s. Shown are a single frame and kymographs from a representative time series.

c, EGFP-Rab5c$^{+/+}$ cells were treated with lentivirus containing control shRNA or shRNA specific for RN-tre. Left: The depletion efficiency of RN-tre mRNA was measured by qPCR (n = 4 independent experiments; mean ± SD). Middle and right: Control or RN-tre-KD cells were transfected with either Vps9-Halo-CAAX (middle) or Rabex5-Halo-CAAX (right), and then imaged by spinning-disk confocal microscopy. Images show that Vps9-Halo-CAAX and Rabex5-Halo-CAAX fail to recruit EGFP-Rab5c to the plasma membrane in RN-tre–depleted cells.

Experiments were repeated three (**a**, **b**) or four times (**c**) with similar results. Scale bars, 5 μm in (**b**), and 10 μm in (**a**) and (**c**). Source numerical data are available in source data.


a
EGFP-Rab5c+/+
mScarlet3-PH(PLCδ1)-Aux1
Clathrin-670nano+/+
Merge
1084 950 558 315
Relative intensity
1.0
0.5
0
20-38.5
40-58.5
60-78.5
80-100
Lifetime cohort (s)
b
EGFP-Rab5c+/+ mCherry-FKBP-OCRL Rabex5-Halo-CAAX
PI(4,5)P2
OCRL
PI4P
0
60
180
360 (s)
Time
EGFP-Rab5c+/+ mCherry-FKBP-OCRL(D523G) Rabex5-Halo-CAAX
PI(4,5)P2
OCRL (D523G)
PI4P
EGFP-Rab5c+/+ mCherry-FKBP-OCRL Rabex5(D313A)-Halo-CAAX
PI(4,5)P2
OCRL
PI4P
c
EGFP-Rab5c+/+ mCherry-FKBP-OCRL-Sac1 Vps9-Halo-CAAX
PI(4,5)P2
PI4P
OCRL -Sac1
PI
EGFP-Rab5c+/+ mCherry-FKBP-OCRL-Sac1-dead Vps9-Halo-CAAX
PI(4,5)P2
PI4P
OCRL (D523G) -Sac1 (C392S)
PI
d
EGFP-Rab5c+/+ mCherry-FKBP-PTEN Vps9-Halo-CAAX
PI(3,4,5)P3
PTEN
PI(4,5)P2
e
Rabex5-mEGFP+/+ mCherry-FKBP-OCRL Halo-PH(PLCδ1)
PI(4,5)P2
OCRL
PI4P
f
PC
PI(4,5)P2
Top
Bottom
kD
25
anti-Rab5c
anti-His
g
Control
Lowe syndrome
mEGFP
mEGFP
mEGFP-OCRL
anti-EEA1
Number of spots per um2
0.04
0.03
0.02
0.01
0
ns
****
****
Control mEGFP
Lowe syndrome mEGFP
Lowe syndrome mEGFP-OCRL

Supplementary Fig. 10. PI(4,5)P_2 impedes the recruitment of Rab5 to Rabex5- or Vps9-mistargeted plasma membrane.

a, EGFP-Rab5c$^{+/+}$ clathrin-670nano$^{+/+}$ cells were transiently transfected with the clathrin-specific PI(4,5)P_2 sensor mScarlet3-PH(PLCδ1)-Aux1, and then imaged by TIRF microscopy every 1 s for 300 s. Shown are a single frame from a representative time series and the intensity-lifetime cohorts from 20 cells (mean ± SEM).

b, EGFP-Rab5c$^{+/+}$ cells co-expressing LYN11-FRB-ECFP together with the specified mCherry- and Halo-tagged plasmids were imaged at 15-s intervals by spinning-disk confocal microscopy. Rapamycin was added (set as 0 s) during continuous imaging to trigger the acute recruitment of the mCherry-tagged phosphatases (lower left image at each time point) from the cytosol to the plasma membrane. Kymographs (right panels) were generated along the line on the first image of each montage. The lipid composition change induced in each experiment is illustrated on the left.

c, **d**, EGFP-Rab5c$^{+/+}$ cells co-expressing LYN11-FRB-ECFP together with the specified mCherry-tagged and Halo-tagged plasmids were treated, imaged, and presented as in (**b**).

e, Rabex5-mEGFP$^{+/+}$ cells co-expressing LYN11-FRB-ECFP, mCherry-FKBP-OCRL, and the PI(4,5)P_2 sensor Halo-PH(PLCδ1) were imaged at 20-s intervals by spinning-disk confocal microscopy. Rapamycin was added (set as 0 s) during continuous imaging.

f, Rab5c bound to His-Vps9-liposomes without or with 2% PI(4,5)P_2 was floated to the top of the sucrose gradient. His-Vps9 was tethered to liposomes via the His-Ni^{2+}-NTA interaction. Western blot analysis of Rab5c and His-Vps9 in the five collected fractions. The presence of His-Vps9 in the top fraction confirms the successful flotation of His-Vps9-liposomes.

g, De-identified Lowe syndrome patient fibroblasts and control fibroblasts were transfected with either mEGFP-OCRL or a vector containing mEGFP alone. The cells were then stained for endogenous EEA1 and imaged using spinning-disk confocal microscopy. Numbers of identified EEA1-labeled endosomes are shown on the right (mean ± SEM; n = 25, 21, and 21 cells). Statistical analysis was performed using the ordinary one-way ANOVA with Tukey's multiple comparisons test; ****$P < 0.0001$; ns, not significant.

Experiments were repeated twice (**c**, **d**) or three times (**a**, **b**, **e**-**g**) with similar results. Scale bars, 5 μm in (**a**), and 10 μm in (**b**-**e**) and (**g**). Source numerical data are available in source data.